Proceedings 10th NUMGE 2023
10th European Conference on Numerical Methods in Geotechnical Engineering
Zdravkovic L, Kontoe S, Taborda DMG, Tsiampousi A (eds)

https://doi.org/10.53243/NUMGE2023-88

Impact of cyclic degradation of soil properties on the performance of monopile foundations for offshore wind turbines: a qualitative numerical study

M. D'Ignazio[1,2] , C. Molina Mesa[3], M. Kanitz[4] , A. Cortez[4], S. M. Bascuñán Chaparro[4]

[1]*Department of Civil Engineering, Tampere University, Tampere, Finland*
[2]*Ramboll Finland Oy, Tampere, Finland*
[3]*Rambøll Denmark, Copenhagen, Denmark*
[4]*Ramboll Germany, Hamburg, Germany*

ABSTRACT: Monopile foundations for offshore wind turbines experience significant cyclic loading originating from wind and waves. Degradation of soil properties under cyclic loading will likely impact the monopile behaviour and, therefore, this shall be accounted for in design. Among the different approaches used to evaluate cyclic degradation, cyclic contour diagrams provide information on both soil stiffness and shear strength degradation with number of cycles. Cyclic properties from contours are based on strain or pore pressure accumulation under storm loading and relevant load ratios. The paper investigates the impact of cyclic degradation of soil properties on the performance of monopiles by 3D FEA. The study is carried out for ideal soil profiles and for a given large diameter monopile geometry. Input parameters are established from databases. The aim is to qualitatively evaluate different assumptions when modelling cyclic degradation to provide insights into the impact of cyclic loading on monopile behaviour.

Keywords: monopile; cyclic degradation; PLAXIS 3D; contour diagrams; offshore wind

1 INTRODUCTION

The design of offshore wind turbine (OWT) monopile foundations is influenced by the effect of cyclic loading that originates from wind and waves. Cyclic loading on offshore structures and, therefore, foundations, often results in changes of soil properties due to accumulation of strain and/or pore pressure (e.g., Andersen, 2015). Degradation of soil properties (i.e., shear strength and moduli) will affect both the capacity and the displacements. Therefore, cyclic effects shall be accounted for in design to ensure that the tolerable pile displacements are not exceeded.

Jostad et al. (2023) showed how neglecting cyclic effects in monopile design may lead to nonconservative results in terms of ULS check. They demonstrated how a PISA (Byrne et al., 2019) type analysis assuming monotonic soil curves would lead to a lower L/D ratio (L=pile length; D=pile diameter) compared to a full 3D PDCAM (Jostad et al., 2015) analysis including cyclic effects as well as partial drainage in sandy soil.

Full 3D cyclic analyses are generally not feasible in most commercial projects of wind farms that include several turbines, where OWT foundation design is carried out for each turbine and for a location-specific soil profile. Therefore, engineering assumptions play a key role in establishing simplified cyclic degradation approaches.

The API (API, 2014) guidelines include analytical methods to account for cyclic degradation below foundations or along piles. The cyclic degradation factors are then applied to the soil support springs. Nevertheless, the API soil support springs were developed for long slender piles and are not suitable for the short and stiff large-diameter piles that are encountered nowadays.

Soil contour diagrams (e.g. Andersen, 2015) represent a practical and comprehensive tool to derive cyclic soil properties for different combinations of average and cyclic stresses and strains at different number of cycles. Contour diagrams are based on numerous laboratory tests including cyclic direct simple shear (DSS) as well as cyclic triaxial compression (TXC) and extension (TXE) tests. One drawback of contour diagrams is that their construction requires a large number of tests. Nevertheless, cyclic soil properties can be estimated from existing databases according to basic soil properties such as relative density, fines content, over consolidation ratio, plasticity index and shear strength (Andersen et al., 2023).

Once a contour diagram is selected for a given soil unit, cyclic degradation can be estimated at any cycle *N*. For monopiles, the distribution of *N* with depth resulting

from distribution of cyclic shear stresses along the pile will impact the soil's stiffness and failure criterion and, therefore, the structural performance. To the Authors' knowledge, there is no unique and well-accepted method for modelling cyclic strength variation along monopiles.

This paper aims to illustrate qualitatively the effects of cyclic degradation of soil properties on monopile performance, in terms of pile displacements for different soil profiles and assumptions on cyclic effects around the monopile. The analyses are carried out using the Finite Element software PLAXIS 3D Connect Edition V21 for a large diameter monopile geometry that is frequently encountered in current geotechnical practice. Both sandy and clayey soils are considered. Input parameters are based on literature contour diagrams (Andersen, 2004; Andersen, 2015). The calculation scenarios considered assume monotonic strength profile, fully degraded soil profile and partially degraded soil profile. The implications from the different approaches in terms of pile performance are discussed.

2 FINITE ELEMENT ANALYSIS

2.1 Geometry and mesh

The finite element model used in this study is illustrated in Figure 1. Only half of the model is used due to symmetry. The basic geometry concept and boundaries are based on Cortez (2021). The monopile has an outer diameter D=8 m and is embedded 32 m in the seabed (L/D=4), instead of the original 40 m (L/D=5) in Cortez (2021). The updated pile penetration is to account for a more frequently seen L/D ratio in current geotechnical practice. The model is 25D=200 m long. Width and depth are set to 10D=80 m. The bottom of the model is fully fixed, while the lateral boundaries are only fixed normally.

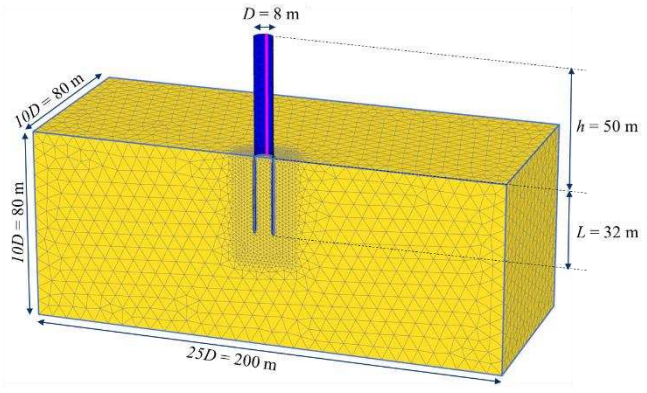

Figure 1. FE geometry and mesh (modified after Cortez, 2021).

The monopile is modelled as a linear elastic plate element with Young's modulus E=210 GPa, Poisson's ratio ν=0.3, considering a constant wall thickness t = 0.1 m (Cortez, 2021). Interface elements are modelled between the soil and the monopile. The FE mesh consists of 10-noded tetrahedral elements. A very fine mesh is used, with mesh refinement in the soil surrounding the monopile.

2.2 Load history and accumulation procedure

The load history considered in this study is based on the 35-hour storm load sequence at 30 m water depth in the North Sea by Bechynski et al. (2019) and the idealized load composition with increasing constant cyclic load amplitude established by Jostad et al. (2023) for the 1-hour peak history. The effects of cyclic degradation of soil properties and, therefore, the coupling between seabed loads and foundation stiffness are neglected in the analyses.

The maximum cyclic bending moment at seabed during idling is 371.5 MNm (Jostad et al., 2023). In the calculation, a horizontal force of 7.43 MN is applied at 50 m above seabed. The average loads are neglected for simplicity. The load history is presented in Table 1.

Table 1. Load parcels of bending moment at seabed (Jostad et al., 2023).

Parcels	Cycles	Storm moment M (MN m)	Load ratio
1	421	18.6	0.05
2	209	55.7	0.15
3	218	92.9	0.25
4	142	130.0	0.35
5	79	167.2	0.45
6	38	204.3	0.55
7	19	241.5	0.65
8	11	278.6	0.75
9	2	306.5	0.825
10	2	325.1	0.875
11	1	343.7	0.925
12	1	371.5	1

The load history in Table 1 is used to determine the soil strength degradation via accumulation procedure (Andersen, 2015). The accumulation procedure determines the combination of a single load with an equivalent number of cycles (N_{eq}) that results in the same level of soil degradation as the entire design cyclic load event.

There are some significant differences between strategies applied to sandy materials and clays. Sand contour diagrams include both pore water pressure development and cyclic strain, where the shear stresses are normalised by a reference stress ($\sigma'_{ref}=100(\sigma'_{vc}/100)^n$, with σ'_{vc}=vertical consolidation stress and n=0.9 (Andersen, 2015)). Diagrams for pore water pressure are then used for accumulation procedure. For clayey soils, the contour diagrams are constructed only for shear strain development and shear stresses are normalised by the undrained static shear strength s_u.

For the accumulation procedure, load parcels are applied in order of ascending amplitude and the storm load is scaled until failure, resulting in an equivalent number of cycles N_{eq} that defines strength degradation.

For a given $N=N_{eq}$, a corresponding stress-strain curve can be extracted from contour diagrams for a given load ratio τ_a/τ_{cy}. Under symmetric two-way loading ($\tau_a/\tau_{cy}=0$), the soil fails faster and reaches the highest deformation within the lowest number of cycles. The symmetric two-way loading is thus considered as the least favourable loading condition, contributing the most to the cyclic soil degradation. In practice, monopile idling after shut-down could represent a two-way loading situation, with negligible average load component.

The results of the accumulation procedure are presented in Sections 2.3 and 2.4. Note that for purely qualitative illustration purposes, the global load history at seabed in Table 1 is used to calculate N_{eq}. In reality, the load history is redistributed along the pile and could possibly result in larger N_{eq} at shallow depth.

2.3 Cyclic soil properties of sand

The selection of cyclic material properties for sand are based on the cyclic contour database in Andersen (2015) and the contour selection procedure described in Andersen et al. (2023). For simplicity, only DSS contour diagrams are considered.

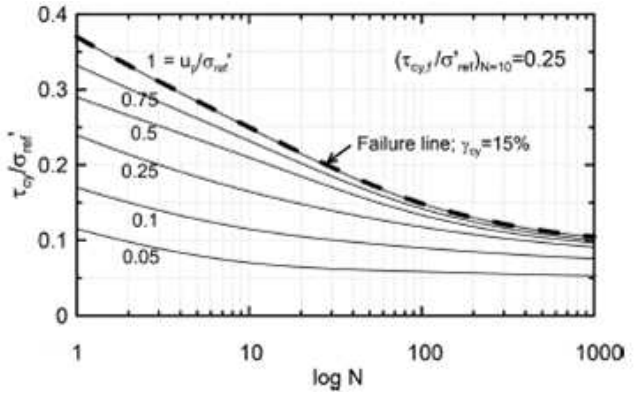

Figure 2. DSS pore pressure contours for $\tau_a=0$ on normally consolidated sand and silt with $(\tau_{cy}/\sigma'_{ref})_{N=10}=0.25$ (Andersen, 2015).

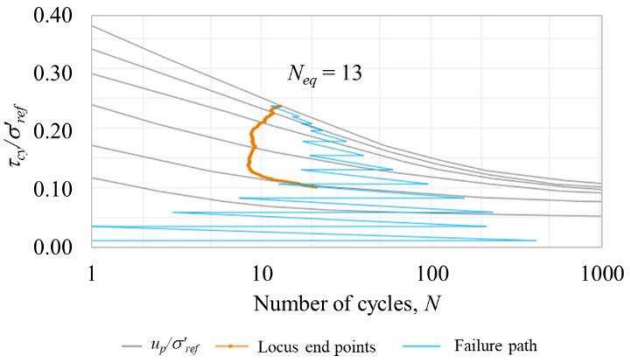

Figure 3. Pore pressure accumulation for $(\tau_{cy}/\sigma'_{ref})_{N=10}=0.25$ and $\tau_a=0$ DSS diagram from Andersen (2015) and load history of Table 1.

For this study, a contour diagram for normally consolidated sand with cyclic DSS strength τ_{cy}/σ'_{ref} = 0.25 at N=10 cycles for symmetric (two-way) loading (i.e., average stress τ_a=0) is selected. According to Andersen (2015), $(\tau_{cy}/\sigma'_{ref})_{N=10}$= 0.25 would be representative of a sand with a relative density D_r≈70-80%, fines content between 5 and 20% and friction angle ϕ'≈37° (τ_a/σ'_{ref} ≈0.75). The τ_{cy}/σ'_{ref} vs N pore pressure contour diagram is presented in Figure 2.

Figure 3 shows the results of the pore pressure accumulation procedure, carried out with the UDCAM-S cyclic accumulation tool in PLAXIS. Fully undrained conditions are assumed. The calculation led to an equivalent number of cycles at failure N_{eq}=13. For N_{eq}=13, τ_{cy}/σ'_{ref}=0.24. The calculated N_{eq} could possibly be lower if partial drainage during accumulation is accounted for (Andersen, 2015; Jostad et al., 2023).

2.4 Cyclic soil properties of clay

The selection of cyclic material properties for clay are based on the cyclic contour diagrams for Drammen clay in Andersen (2004) and the contour selection procedure described in Andersen et al. (2023). For simplicity, only DSS contour diagrams are considered.

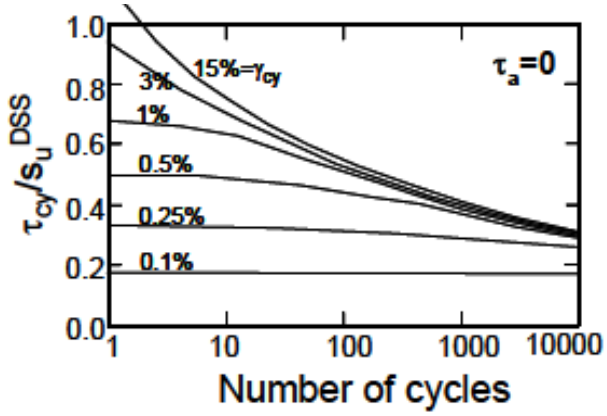

Figure 4. DSS strain contour diagram for Drammen Clay OCR=4 (Andersen, 2004).

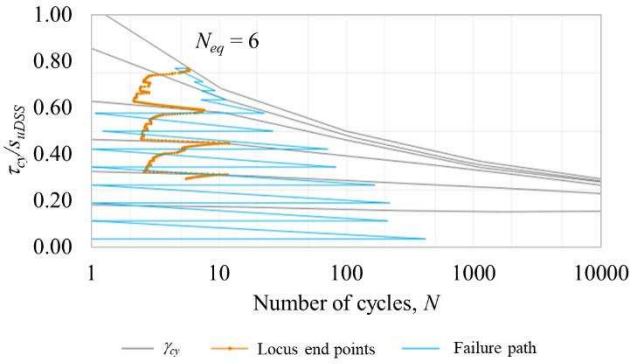

Figure 5. Shear strain accumulation for Drammen Clay OCR=4 DSS diagram from Andersen (2004) and load history of Table 1.

For this study, the OCR=4 contour diagram for symmetric (two-way) loading (i.e., average stress τ_a=0) is used. For OCR=4, s_{uDSS}/σ'_{vc}=0.67. The contour diagram is presented in Figure 4.

Figure 5 shows the results of the strain accumulation procedure, carried out with the UDCAM-S cyclic accumulation tool in PLAXIS. Fully undrained conditions are assumed. The calculation led to an equivalent number of cycles at failure N_{eq}=6. For N_{eq}=6, τ_{cy}/s_{uDSS}=0.85.

2.5 NGI-ADP constitutive model

The NGI-ADP soil model (Grimstad et al., 2012) is a total stress elastoplastic model based on an anisotropic Tresca failure criterion. The anisotropic behaviour follows the ADP framework, where the s_u profiles for active (A), direct simple shear (D), and passive (P) stress paths are given directly as input parameters. The nonlinear hardening curves are described by input of the peak s_u and corresponding shear strains (γ_A, γ_{DSS} and γ_P) in the three directions of shearing represented by triaxial compression, DSS, and triaxial extension. By interpolation between the three input curves, the model determines the anisotropic behaviour of the clay for a general three-dimensional (3D) stress state.

Undrained triaxial and DSS tests are required to establish input parameters. The model simulates an initial anisotropic consolidation stress state by means of the initial shear mobilization parameter τ_0/s_{uA}. The initial inclination of the stress-curves comes from the initial shear modulus G_0, which also defines the unloading/reloading modulus (G_{ur}) and the magnitude of the elastic strain components.

The model assumes that s_u varies linearly with depth within a soil layer. A constant s_{uAref} (reference active or triaxial compression) at a reference depth y_{ref}, together with a strength increase parameter s_{u_incA}, defines the s_u profile in the soil layer. Above y_{ref}, s_{uA} is constant and equal to s_{uAref}. The strength profiles for DSS and passive (triaxial extension) are defined from the anisotropy ratios s_{uDSS}/s_{uA} and s_{uP}/s_{uA}.

2.6 Calibration of NGI-ADP model and input parameters

Constitutive model parameters are calibrated using the SoilTest tool in PLAXIS. The monotonic and cyclic DSS curves are extracted from contour diagrams for load ratios τ_{cy}/τ_a=0 and τ_a/τ_{cy}=0, respectively. The τ_a=0 cyclic curves are selected in line with the maximum cyclic bending moment at seabed during idling, assuming little or no average stress component. Figures 6 and 7 illustrate the monotonic and cyclic DSS curves versus the NGI-ADP model.

Table 2 summarizes the NGI-ADP input parameters for sand and clay. The undrained shear strength profiles for s_{uA}=s_{uD}=s_{uP} are defined assuming homogeneous soil conditions.

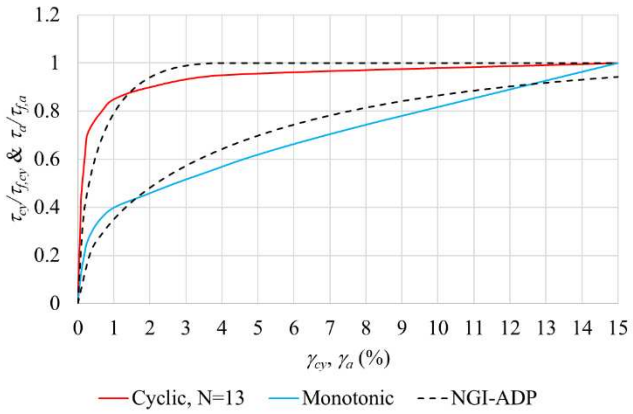

Figure 6. Normalized DSS static (monotonic) and cyclic (two-way loading) curves for normally consolidated sand with (τ_{cy}/σ'_{ref})$_{N=10}$=0.25 versus NGI-ADP model.

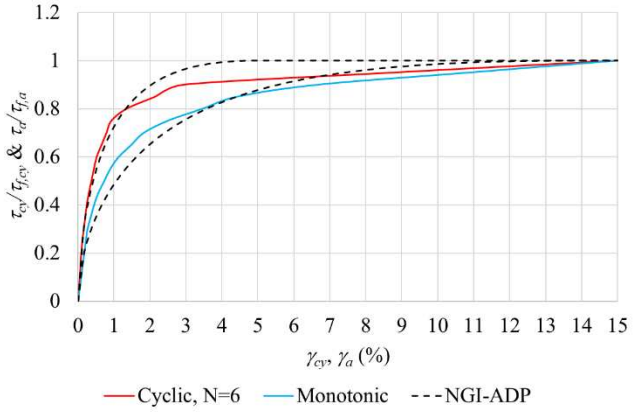

Figure 7. Normalized DSS static (monotonic) and cyclic (two-way loading) curves for Drammen clay OCR=4 versus NGI-ADP model.

Table 2. Input parameters for NGI-ADP model.

Parameter	Unit	Sand (Static)	Sand (cyclic, N=13)	Clay (Static)	Clay (cyclic, N=6)
γ'	kN/m^3	10	10	10	10
G_{ur}/s_u	-	1500	1500	750	750
γ_A	-	30	4	14	5
γ_{DSS}	-	30	4	14	5
γ_P	-	30	4	14	5
τ_0/s_{uA}	-	0	0	0	0
s_{uA}	kPa	5	1	1	1
s_{uA} *inc.*	kPa/m	6.5	2.1	6.7	5.7
y_{ref}	m	0	0	0	0
s_{uDSS}/s_{uA}	-	1.0	1.0	1.0	1.0
s_{uP}/s_{uA}	-	1.0	1.0	1.0	1.0
ν_u	-	0.495	0.495	0.495	0.495
K_0	-	1.0	1.0	1.0	1.0
R_{inter}	-	1.0	1.0	1.0	1.0

2.7 Calculation scenarios and procedure

The calculations are carried out as undrained push-over analyses of the monopile, with a horizontal load H=7.43 MN applied 50 m above the seabed, resulting in a bending moment of 371.5 MNm at seabed, in agreement with Table 1.

Three different calculation scenarios are evaluated for both sand and clay profiles:

- *Scenario 1*: Static (monotonic) soil strength (no degradation)
- *Scenario 2*: Cyclic soil strength over the entire soil profile for N=13 (sand) and N=6 (clay)
- *Scenario 3*: Cyclic soil strength up to 15 m depth below seabed. Below 15 m depth, static soil strength (no degradation).

The threshold 15 m depth is selected based on engineering judgement, assuming that below that depth, cyclic utilization will not induce failure in the soil regardless of the number of applied cycles. In reality, the threshold depth will change along with shear stress redistribution resulting from the application of the different cyclic load parcels. For simplicity, and for the sake of purely qualitative comparison, it is then assumed that no strength or stiffness degradation occurs below 15 m below seabed. Possible strength degradation at the monopile's base is also neglected.

3 RESULTS AND DISCUSSION

Figures 8 and 9 illustrate the horizontal load (H) applied at 50 m above seabed versus pile displacement at seabed y for sand and clay profiles, respectively.

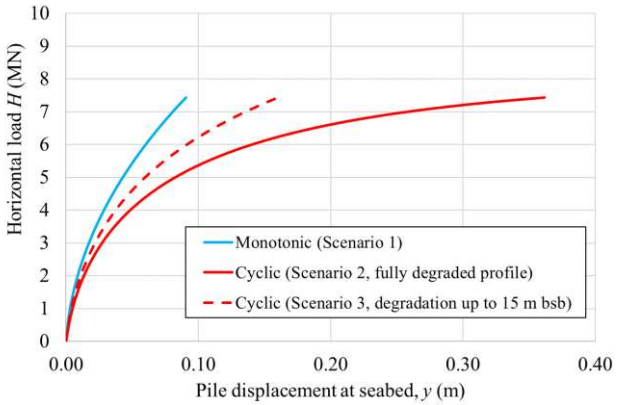

Figure 8. Horizontal load at 50 m above seabed vs pile displacement at seabed y (sand).

Neglecting pore pressure build up in sand due to cyclic loading might underestimate the monopile deformations and possibly reduce the required target penetration depth (Figure 8). Nevertheless, assuming a fully degraded soil profile along the entire monopile length might add unnecessary conservativism and possibly result in an oversized structure. Optimal design shall be based on a thoughful modelling of cyclic strength versus depth along the monopile.

Strain accumulation and cyclic degradation appear to have a lower impact in clay (Figure 9), at least for the calculated N_{eq}=6. In clay, cyclic loading may even produce a positive effect, as τ_{cy}/s_{uDSS} can be higher than 1 at low N because of rate effects, as reported by Andersen (2004) for normally consolidated Drammen clay.

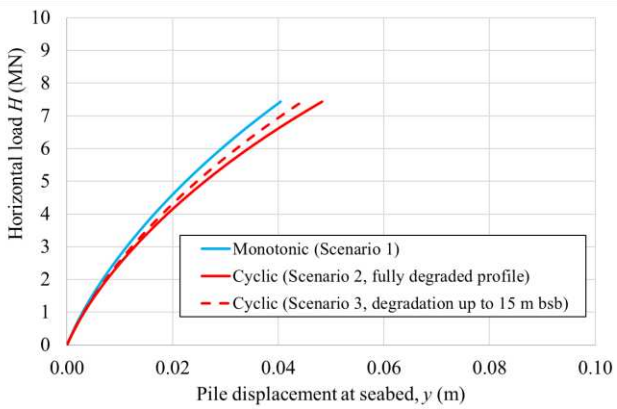

Figure 9. Horizontal load at 50 m above seabed vs pile displacement at seabed y (clay).

In previous studies, it was shown how N_{eq} and strength degradation vary along the monopile, with N_{eq} typically decreasing with depth, i.e., degradation of soil properties being more severe at shallow depths due to higher soil utilization and load redistribution (e.g. Jostad et al., 2014; Zhang et al., 2017). However, a detailed derivation of N_{eq} vs depth may require advanced cyclic FEA using UDCAM/PDCAM models (Jostad et al., 2014; Jostad et al., 2015; Jostad et al., 2023), where the full load history is applied and N_{eq} calculated at each integration point within the soil domain considering stress redistribution as well as drainage conditions. Alternatively, an iterative beam or FE analysis can be carried out in which the cyclic parcels are evaluated one by one with a step-wise update of stiffness and strength properties (e.g. Zhang et al., 2017; Jostad et al., 2023).

4 CONCLUSIONS

This study illustrated the impact of cyclic degradation of soil properties on the performance of a large diameter monopile (L/D=4) by 3D FEA. The study was carried out for ideal sand and clay profiles and for different scenarios assuming: undegraded, fully degraded and partially degraded soil profiles along the monopile. Input parameters were established from an existing database of cyclic contour diagrams. The strength and stiffness degradation were assessed based on DSS stress-strain curves obtained for an equivalent number of cycles N_{eq}, resulting from pore pressure and shear strain accumulation procedure for a given idealized North Sea storm load history.

The FE analyses showed how neglecting pore pressure build up in sand due to cyclic loading might result in unconservative design. The effect appears to be less pronounced in clay, especially at low *N*. On the other hand, assuming a fully degraded soil profile along the entire monopile length (i.e., cyclic strength based on N_{eq} at failure from strain or pore pressure accumulation) might end up in an overconservative design. Optimal monopile design shall be based on a careful modelling of cyclic strength versus depth along the monopile, assuming redistribution of shear stresses along the pile resulting from the application of cyclic load parcels, as also indicated in the literature. Simplified approaches shall account for the distribution of strain, pore pressure and number of cycles along the monopiles based on engineering based criteria. For instance, by identifying a threshold depth below which cyclic degradation is anticipated to play a minor role; or by modelling a depth dependent N_{eq} associated with a cyclic failure criterion. Moreover, including partial drainage in the pore pressure accumulation procedure will likely result in lower N_{eq}.

The results and the procedure presented in this study are meant to illustrate qualitatively the impact of cyclic loading on monopile behaviour and shall not be used directly in design.

5 ACKNOWLEDGMENTS

This Authors would like to thank Jan Dührkop from Ramboll for the useful discussions on the topic treated in this paper.

6 REFERENCES

Andersen, K. H. 2004. Cyclic clay data for foundation design of structures subjected to wave loading. *In Cyclic behaviour of soils and liquefaction phenomena,* 371-387.

Andersen, K. H. 2015. Cyclic soil parameters for offshore foundation design. *In Frontiers in offshore geotechnics III*, 5, London, Taylor &Francis.

Andersen, K. H., Engin, H. K., D'Ignazio, M., Yang, S. 2023. Determination of cyclic soil parameters for offshore foundation design from an existing data base. *Ocean Engineering*, **267**, 113180.

API (American Petroleum Institute), 2014. Recommended practice 2AWSD planning, designing and constructing fixed offshore platforms - Working stress design. 22nd ed. Washington, DC: API.

Bachynski, E. E., Page, A., Katsikogiannis, G. 2019. Dynamic response of a large-diameter monopile considering 35-hour storm conditions. *In Vol. 58899 of Proc., Int. Conf. on Offshore Mechanics and Arctic Engineering*. Reston, VA: ASCE.

Byrne, B. W., et al. 2019. PISA design methods for offshore wind turbine monopiles. *In Proc., Offshore Technology Conf. Boca Raton*, FL: CRC Press Offshore Technology Conference.

Cortez, A. 2021. Zur Anwendung erweiterter Stoffmodelle für undräniertes zyklisches Bodenverhalten in der Offshore-Pfahlbemessung. Masterarbeit, Technische Universität Hamburg. (In German. Title in English: Advanced soil models for undrained cyclic soil behaviour applications in offshore pile design)

Grimstad, G., Andresen, L., Jostad, H.P. 2012. NGI-ADP: Anisotropic shear strength model for clay. *International Journal for Numerical and Analytical Methods in Geomechanics* **36(4),** 483–497.

Jostad, H. P., Grimstad, G., Andersen, K. H., Saue, M., Shin, Y., You, D. 2014. A FE procedure for foundation design of offshore structures–applied to study a potential OWT monopile foundation in the Korean western sea. *Geotech. Eng. J. SEAGS AGSSEA* **45(4)**, 63–72.

Jostad, H. P., Grimstad, G., Andersen, K. H., Sivasithamparam, N. 2015. A FE procedure for calculation of cyclic behaviour of offshore foundations under partly drained conditions. *In Frontiers of Offshore Geotechnics III*, 1, 153–172.

Jostad, H. P., Liu, H., Sivasithamparam, N., Ragni, R. 2023. Cyclic Capacity of Monopiles in Sand under Partially Drained Conditions: A Numerical Approach. *Journal of Geotechnical and Geoenvironmental Engineering*, **149(2)**, 04022129.

Zhang, Y., Andersen, K. H., Jeanjean, P., Mirdamadi, A., Gundersen, A. S., Jostad, H. P. 2017. A framework for cyclic py curves in clay and application to pile design in GoM. *In OSIG SUT conference* (Vol. 2017).